Article

Intermolecular Hydrogen Bonding Directed by Aryl−Perfluoroaryl π−π Stacking Interactions

Jan Alfuth, Katarzyna Kazimierczuk, Tadeusz Połoński, and Teresa Olszewska*
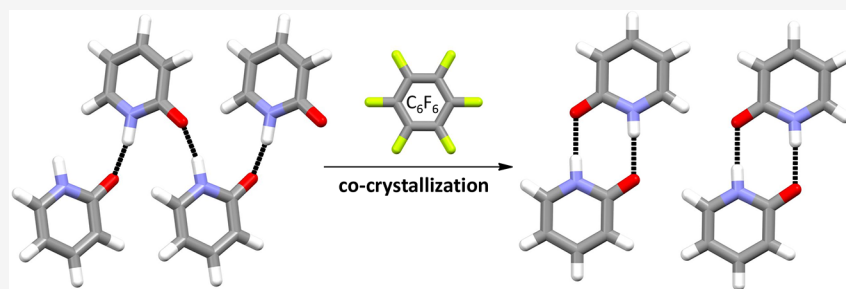
Read Online

ACCESS | Metrics & More | Article Recommendations | Supporting Information

ABSTRACT: The crystal structures of five compounds capable of forming self-complementary hydrogen bonds but crystallizing as catemers or creating more complex crystal structures were compared with those of their complexes prepared by cocrystallization with perfluoroaryl compounds. The results of X-ray diffraction revealed that in all the cases, the π−π stacking interactions caused the reorganization of hydrogen bonds and induced the creation of the expected self-complementary hydrogen bond dimeric motifs. The results point to the potential of aryl−perfluoroaryl interactions for the control of molecular self-assembly of aromatic compounds able to form hydrogen bonds. Also, the electrostatic potential (ESP) surfaces were investigated in terms of intermolecular interactions in the studied cocrystals. The values of the locally most negative and most positive ESP confirmed the best donor and acceptor sites for hydrogen bonding and other contacts.

INTRODUCTION

The rational design and preparation of crystalline molecular solids rely on control of the molecular arrangement using secondary bonding interactions rather than covalent bonding. Hydrogen bonds (HBs) and π−π stacking interactions are crucial in the construction of materials with the desired structure and function.[1−6] Because HBs are generally stronger and more directional than other types of molecular interactions, they are vital for the control of self-assembly, orientation, and aggregation processes in the solid state.[7−13] Therefore, identification and understanding of the preferential formation of specific types of HB arrays are indispensable to predict and rationalize the structural properties of organic molecular crystals.[14−16] On the other hand, weaker non-covalent interactions, like π−π stacking between aromatic units, also play a significant role in crystal engineering because of their ability to control the relative orientation of molecules toward each other in the solid state.[17−22] The principal modes of the arene−arene interaction are T-shaped edge-to-face and slipped face-to-face contacts. However, it is well-known that perfluoro-substitution at one aromatic ring causes domination of the face-to-face interaction mode[23−25] due to the dispersion and quadrupolar interactions between electron-rich and electron-deficient aromatic rings.[26−28] The electron-deficient regions of perfluorinated rings are now commonly referred to as π-holes.[29,30] Consequently, the stacking interactions can also be viewed as an interaction of such a π-hole with aromatic rings. The arene−perfluoroarene stacking interaction emerges as a reliable and robust synthon with potential utility in supramolecular chemistry,[31−33] crystal engineering,[34−38] discotic liquid crystals,[39] solid-state reactions,[40] and biomolecular interactions in solution.[41]

The majority of the reported crystallographic studies have dealt with cocrystals of aromatic hydrocarbons and perfluoro-carbons.[35−38] Much less research has been done on cocrystals of compounds bearing functional groups.[42−47] Moreover, the competition or cooperation between hydrogen bonding and π−π stacking interactions in molecular self-assembly has been identified as a useful effect in crystal engineering.[48−52] For example, we have recently shown that cocrystallization of star-shaped triaryl compounds with pentafluorophenol induces the formation of hydrogen-bonded cyclic trimers due to aryl−perfluoroaryl stacking interactions.[53]

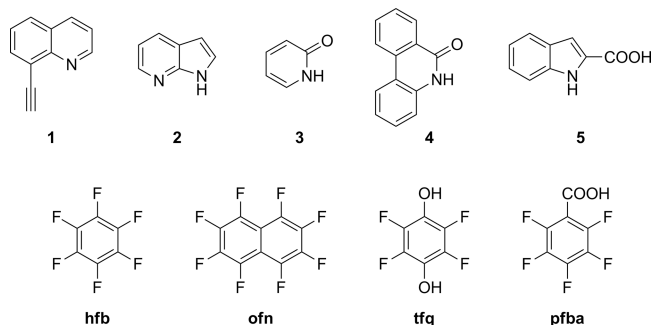In this context, we were curious about whether $\pi-\pi$ stacking interactions could help to control the supramolecular assembly via HBs. As the first example, we chose 8-ethynylquinoline (**1**, Scheme 1), which was expected to form dimers due to self-

Scheme 1. Chemical Structures of Compounds 1−5 and the Perfluoroarenes Used in the Study

complementary ≡C−H···N interactions in the form of a $R_2^2(12)$ motif (**I**, Scheme 2). However, the crystal structure of **1**

Scheme 2. Expected (I) and Observed (II) Supramolecular Motif in the Crystal Structure of 1
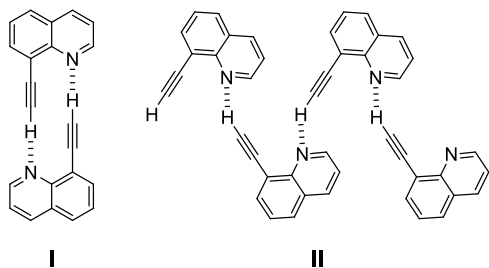
revealed the catemer $C(6)$ motif (**II**) instead of the cyclic motif **I**. Much to our delight, the situation was reversed upon cocrystallization of **1** with hexafluorobenzene (**hfb**) that caused the self-assembly of molecules of **1** into dimers **I**. Thus, we searched for more examples of compounds crystallizing in rather uncommon packing modes instead of creating self-complementary HBs using popular supramolecular synthons. In this account, we investigated the crystal structures of compounds **1−5** before and after their complexation with perfluoroaryl derivatives such as hexafluorobenzene (**hfb**), octafluoronaphthalene (**ofn**), tetrafluorohydroquinone (**tfq**), or pentafluorobenzoic acid (**pfba**) (Scheme 1). In all of the above cases, aryl−perfluoroaryl stacking interactions led to a significant reorganization of the intermolecular HBs in the cocrystals containing **1−5**.

■ EXPERIMENTAL METHODS

Synthesis and Crystallization. Compounds **1**[54] and **3**[55] were prepared according to the literature procedures. The remaining substrates were purchased from Sigma-Aldrich, Alfa Aesar, or Apollo Scientific and used without further purification. The cocrystals **1$_2$·hfb**, **2$_2$·hfb**, and **3$_2$·hfb** were prepared by crystallization from hot hexafluorobenzene (**hfb**). Colorless crystals of the complexes are not air-stable and quickly decompose because of the volatility of **hfb**. However, they can be stored for a long time in the mother liquor or in the presence of **hfb** vapor. The cocrystal **4$_2$·ofn** was obtained by slow evaporation of the equimolar solution of the components in THF. The cocrystals with tetrafluorohydroquinone (**tfq**) or pentafluoro-

benzoic acid (**pfba**) were obtained by the same method from DCM−heptane. The details and characterization of the cocrystals are listed in the ESI.

Theoretical Calculations. To obtain molecular electrostatic potential maps of the molecules of the compounds studied, the geometries of the isolated molecules were first optimized using the Gaussian 16 package[56] at the B3LYP/6-31G** level of theory, and then their ESP maps were visualized with GaussView 6.1.1.[57] Frequency calculations were also included to determine whether the true energy minima were obtained. Finally, the maximum and minimum values of the electrostatic potential ($V_{S,max}$ and $V_{S,min}$) on the molecules were calculated.

Crystal Structure Determination. The X-ray diffraction data were collected on an IPDS 2T dual-beam diffractometer (STOE & Cie GmbH, Darmstadt, Germany) at 120.0(2) K with Mo Kα radiation of a microfocus X-ray source (GeniX 3D Mo HighFlux, Xenocs, Sassenage, France, 50 kV, 1.0 mA, λ = 0.71069 Å) for all the structures. Every crystal was thermostated in a nitrogen stream at 120 K using a CryoStream-800 device (Oxford CryoSystems, UK) during the entire experiment. Data collection and data reduction were controlled by the X-Area 1.75 program.[58] The structure was solved by the SHELXT method[59,60] and refined using Olex2[61,62] and SHELX-2015[59,60] program packages. Mercury[63] was used to prepare Figures 1−7. All the nonhydrogen atoms were modeled as anisotropic, whereas the H atoms were refined as isotropic. Hydrogen atoms were placed in idealized positions and refined with the usual restraints of the riding model. In **3·tfq**, the amide moiety (H1−N1−C13−O1) was modeled as disordered (s.o.f. 0.815(6)/0.185(6)). The crystallographic data and some details of the structural refinement are summarized in Table S1 in the ESI. Structural details of the hydrogen bonding are listed in Table 1.

Table 1. Parameters of the Selected Hydrogen Bonds in 1 and Cocrystals of 1−5[a]

	D−H···A	H···A(Å)	D···A(Å)	D−H···A(°)
1	C8−H8···N1^i	2.35	3.199(2)	148
1$_2$·hfb	C11−H11···N1^{ii}	2.42	3.357(5)	167
2$_2$·hfb	N2−H2A···N1^{iii}	2.04	2.911(2)	168
3$_2$·hfb	N1−H1···O1^{iv}	1.91	2.773(1)	176
	C5−H5···O1^v	2.53	3.399(2)	147
4$_2$·tfq	N1−H1···O1^{vi}	2.00	2.833(9)	158
	O2−H2A···O1	2.01	2.829(3)	166
4$_2$·ofn	N1−H1···O1^{vii}	1.92	2.800(5)	177
5$_2$·pfba	O1−H1···O4	1.81	2.638(2)	170
	O3−H3A···O2	1.78	2.607(2)	169
	O5−H5A···O6^{viii}	1.80	2.627(3)	171

[a]Symmetry codes: (i) 1.5 − x, −0.5 + y, 1.5 − z; (ii) 2 − x, 1 − y, 1 − z; (iii) −x, 2 − y, 1 − z; (iv) 1 − x, 1 − y, 1 − z; (v) −1 + x, y, z; (vi) 1 − x, 1 − y, 1 − z; (vii) 2 − x, 2 − y, − z; (viii) 1 − x, − y, 2 − z.

Crystallographic data for all of the structures reported in this paper have been deposited with the Cambridge Crystallographic Data Centre as supplementary publication no. CCDC 2263874, 2263877, 2263878, 2263881, 2263886, 2263888, 2263893, and 2263894. The data can be obtained free of charge from The Cambridge Crystallographic Data Centre (CCDC) via http://www.ccdc.cam.ac.uk/structures.

■ RESULTS AND DISCUSSION

8-Ethynylquinoline (1). Numerous examples of the successful creation of discrete molecular complexes as well as 1D or 2D hydrogen bond networks from alkynyl C−H donors and azaheterocycles have been reported.[64−69] These findings prompted us to investigate the possibility of constructing dimeric structures assembled by self-complementary ≡C−H···N interactions. Thus, we obtained compound **1** and crystal-

lized it from AcOEt. Its crystal structure (monoclinic space group $P2_1/n$) revealed infinite antiparallel polymeric tapes spreading along the direction of [010]. These structures are created with the use of ≡C−H⋯N bonds and connected via face-to-face π-stacking interactions. The distance between the planes of two adjacent molecules of **1** is 3.51 Å. Instead of the expected cyclic synthon **I**, the molecules are connected by linear ≡C−H⋯N HBs creating a catemer structure **II** (Figure 1a).
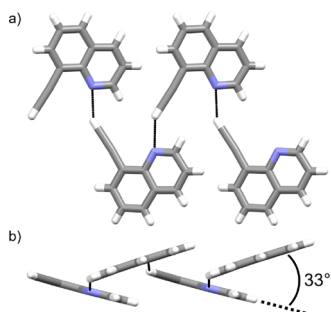

Figure 1. Crystal structure of **1**: (a) top view of a fragment of the tape stabilized by ≡C−H⋯N HBs and (b) side view of the fragment showing the dihedral angle between the molecules of **1**.

The N⋯H distance of 2.35 Å indicates a relatively strong ≡C−H⋯N interaction, even though the C−H⋯N bond angle of 148° is quite far from the linear orientation (Table 1).[68] Furthermore, the dihedral angle between two HB molecules generating the catemer is 33° (Figure 1b), whereas the cyclic synthon **I** requires coplanar orientation of two participating molecules of **1**. Therefore, we came up with the idea that aryl−perfluoroaryl interactions may force two neighboring molecules of **1** into a coplanar orientation and induce the formation of the dimer **I**. Cocrystallization of **1** with hexafluorobenzene (**hfb**) readily afforded 2:1 complex **1₂·hfb**.

It crystallizes in the monoclinic space group $P2_1/c$, and the asymmetric unit contains one molecule of **1** and half of a molecule of **hfb**. The crystal structure of **1₂·hfb** revealed that the molecules of **1** indeed aggregate into dimers in the form of cyclic motif **I**. The dimers are centrosymmetric and essentially planar. The N⋯H distances are 2.42 Å, slightly longer than those in the uncomplexed **1**, but the C−H⋯N angles are this time closer to 180° (Figure 2a, Table 1). Both factors indicate again relatively strong ≡C−H⋯N interactions. The crystals of

the complex are composed of parallel tapes of alternating dimers **I** and **hfb** molecules connected by pairs of C−H⋯F interactions between the aryl and perfluoroaryl units (Figure 2a). It is known that the C−H⋯F interactions are common in crystals and cocrystals of fluoroaromatic compounds.[70] The H⋯F distances in **1₂·hfb** are 2.61 and 2.65 Å, so they are slightly shorter than the sum of the van der Waals radii of H and F (2.67 Å),[71] and the C−H⋯F angles in both cases are approximately 154°. The structure of **1₂·hfb** is further stabilized by π-stacking interactions between the aryl and perfluoroaryl rings of the parallel tapes, which aggregate in a simple brick-wall motif (Figure 2b). The distance between the centroid of an **hfb** molecule and the plane of a quinoline moiety of **1** is 3.34 Å. Moreover, the molecules of each component are almost parallel, as the dihedral angle between the planes of the molecules is ca. 1.4° (Figure 2c).

7-Azaindole (2). Compound **2** (1H-pyrrolo[2,3-b]-pyridine, also known as 7-azaindole) attracts considerable interest in material chemistry as a blue emitter[72] and in the field of drug chemistry.[73] Because of the close relationship with the nucleic purine bases, i.e., adenine and thymine, the self-association of **2** has been the object of numerous experimental and theoretical studies.[74−76] In solution, this aza-aromatic compound forms cyclic dimers **III** joined by a pair of complementary N−H⋯N hydrogen bonds (Scheme 3). In addition to this, in the excited state, dimer **III** undergoes a photoinduced double proton transfer as evidenced by fluorescence spectra.[76]

Scheme 3. Expected (III) and Observed (IV) Supramolecular Motif in the Crystal Structure of 2
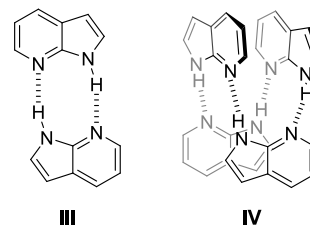
Surprisingly, determination of the crystal structure has revealed that **2** crystallizes as tetramers **IV** with the use of four N−H⋯N HBs (Scheme 3).[77] One of the possible explanations of this behavior is the van der Waals interaction between roughly parallel heteroaromatic rings within tetramer **IV**. Also, in this case, it seemed reasonable to us to assume that a complexation of **2** with a perfluoroaryl compound, leading to stabilization gained by π−π stacking interactions, should favor the creation of the planar dimer **III** in the solid state. Indeed, cocrystallization of **2** with **hfb** resulted in the formation of the crystalline 2:1 complex **2₂·hfb**. Its crystal structure (the monoclinic space group $P2_1/c$) revealed centrosymmetric dimers **III**, where the molecules of **2** are held together by two complementary N−H⋯N HBs with an N⋯H distance of 2.04 Å and an N−H⋯N angle of 168°. The structure of **2₂·hfb** is stabilized by face-to-face stacking interactions between the aryl and perfluoroaryl rings, and the adjacent dimers interact via face-to-edge stacking interactions (Figure 3a). The distance between the centroid of the **hfb** molecule and the plane of the 7-azaindole molecule is 3.36 Å, and the angle between the planes of the molecules is ca. 1.8°. In the cocrystal, sheets composed of molecules of **2** (*A*) and **hfb** (*B*) can be

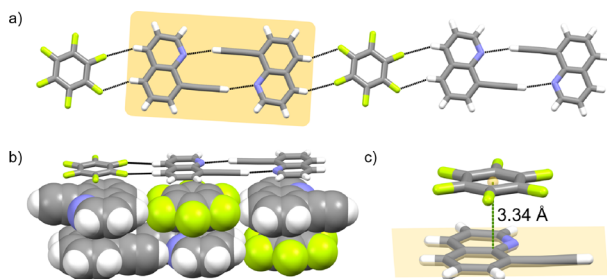**Figure 2.** Crystal structure of **1₂·hfb**: (a) top view of a fragment of the tape composed of alternating dimers **I** and **hfb** molecules (one of the dimers is highlighted in light orange), (b) side view of the molecules stacked in a brick-wall motif, and (c) view of the relative orientation of the **hfb** and **1** molecules, with the distance between the centroid of C_6F_6 and the plane of **1**. HBs indicated by black lines.
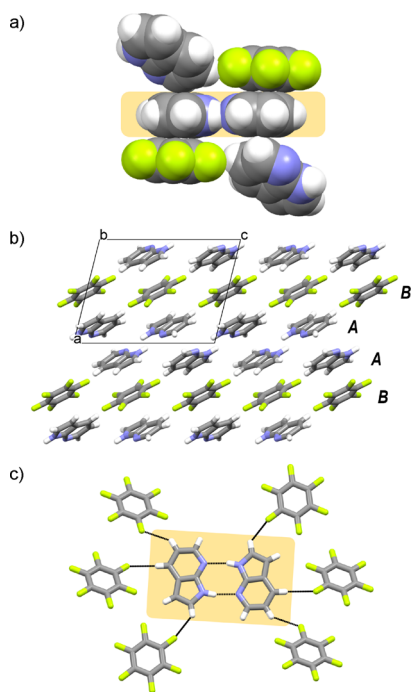
a)

b)

c)

Figure 3. Crystal structure of $2_2\cdot$**hfb**: (a) side view of a fragment of the structure indicating the interactions of 2_2 dimer (highlighted in light orange) with the neighboring molecules, (b) the sheets of molecules of **2** (*A*) and **hfb** (*B*) (view along the *b*-axis), and (c) view of the C−H···F bonds (black lines) between the dimer and the adjacent **hfb** molecules.

distinguished, and they are parallel to (100) and oriented in a $(BAA)_n$ pattern (Figure 3b). Each dimer interacts with as many as six **hfb** molecules through C−H···F HBs (Figure 3c). The average H···F bond length is 2.62 Å.

2-Pyridone (3). Secondary amides assuming *s-cis* conformation (particularly lactams) most often assemble into dimers with the use of self-complementary $R_2^2(8)$ motif **V** (Scheme 4).[8] In fact, self-complementary 2-pyridone (**3**)

Scheme 4. Supramolecular Motifs V−VI Observed in the Crystal Structures of Secondary Amides and the Dimeric Supramolecular Motif VII Characteristic for 2-Pyridone 3
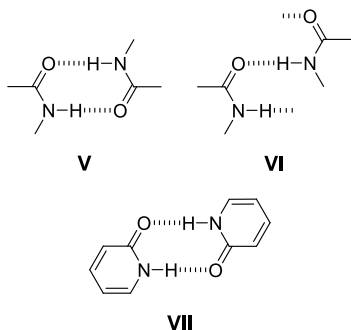
moieties form one of the most reliable and robust hydrogen-bonded dimeric motifs, **VII**, which has found broad application in crystal engineering.[9,78] Surprisingly, the crystal structure of the orthorhombic form of uncomplexed **3** reveals the catemer motif **VI** (puckered chains linked by linear N−H···O=C HBs) instead of the dimers.[79,80] Nevertheless, a recently isolated monoclinic polymorph displayed the dimeric structure **VII**.[81]

As in the previous cases, it seemed reasonable to expect that the addition of a perfluoroaryl component should facilitate the formation of 3_2 self-complementary dimers. The cocrystallization of **3** with **hfb** indeed resulted in the formation of a cocrystal with a 2:1 ratio of the two components ($3_2\cdot$**hfb**). Its crystal structure (monoclinic space group $P2_1/n$) contains the expected amide dimers stabilized by strong and complementary N−H···O=C HBs (Table 1). The arrangement of the amide molecules is similar to that of the monoclinic polymorph of **3**; the dimers are almost planar and connected via weaker C−H···O HBs into undulated ribbons spreading along the *a*-axis (Figure 4a). This time, however, they are
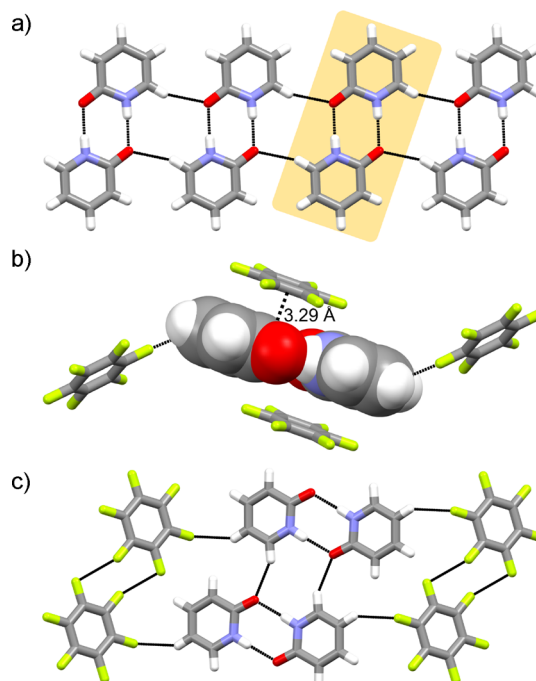
a)

b)

3.29 Å

c)

Figure 4. Crystal structure of $3_2\cdot$**hfb**: (a) top view of a fragment of the undulated ribbon of molecules of **3** (one of the lactam dimers is highlighted in light orange), (b) side view of the dimer with four neighboring **hfb** molecules interacting with it and the distance between the centroid of **hfb** and the plane of **3**, and (c) fragment of the structure depicting the network of HBs and F···F contacts (black lines).

centrosymmetric and separated by **hfb** molecules. In fact, the **hfb** molecules are located not only above and below the ribbons but also on their sides (Figure 4b). The polymeric structures interact with the **hfb** molecules through $\pi-\pi$ stacking interactions and C−H···F HBs. The distance between the centroid of an **hfb** molecule and the plane of a molecule of **3** is 3.29 Å, but the molecules are slightly offset from each other. Also, the two molecules are not cofacial; the dihedral angle between the planes of the molecules is ca. 8°. The observed H···F bond lengths are equal to 2.61 Å and are shorter than the sum of the van der Waals radii of H and F by only 0.06 Å. Additional F···F contacts between the neighboring **hfb** molecules are also present (Figure 4c).

Phenanthridone (4). The aromatic lactam **4** (phenanthridin-6(5*H*)-one) is another example of a secondary *s-cis* amide whose molecules do not form dimers **V** in the solid state. Instead, they aggregate into a polymeric helical structure with the use of linear N−H···O=C HBs (motif **VI**, Scheme

4).[82] Thus, we attempted to control the self-assembly of **4** by crystallizing it with perfluoroaryl compounds.

Because lactam **4** did not form cocrystals with **hfb**, we tried two different methods to generate the dimeric self-assembly of this compound, first by cocrystallization of **4** with tetrafluoro-hydroquinone (**tfq**). The 2:1 cocrystal of **4** with **tfq** (the monoclinic space group $P2_1/c$) is indeed composed of hydrogen-bonded lactam dimers (motif **V**). The length of both the N—H···O=C HBs is 2.00 Å, and the valence angle is equal to 158° (Table 1). The centrosymmetric dimers are not planar; the two molecules of **4** are located on parallel planes separated by ca. 0.72 Å (Figure 5). The amide moiety (H1—
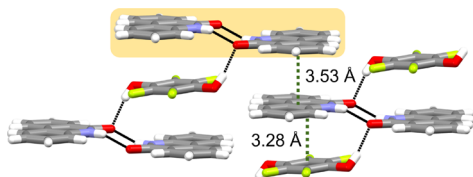

Figure 5. Crystal structure of **4**$_2$·**tfq**: side view of a fragment of the structure with the distances between π-stacked molecules. One of the lactam dimers is colored light orange. HBs are indicated by black lines.

N1—C13—O1) is disordered with a site occupation factor (*s.o.f.*) of 0.815(6)/0.185(6). The dimers are connected by quite unusual O—H···O=C HBs and π−π stacking interactions formed by the **tfq** molecules. The O···H distances are 2.01 Å, and the valence angle of the O—H···O bond is equal to 166°. Offset stacks of the molecules of **4** (C) and **tfq** (D) forming a $(DCC)_n$ pattern can be distinguished (Figure 5). The distance between the centroid of a **tfq** molecule and the plane of the lactam molecule interacting with it is 3.28 Å, whereas the distance between two molecules of **4** is 3.53 Å. The molecules of both components are not parallel; the dihedral angle between the planes constructed for **4** and **tfq** is approximately 5°. We observed additional stabilization via C—H···F and C—H···O HBs as well as face-to-edge π−π stacking interactions between the lactam molecules.

The control of the self-assembly by cocrystallization with **tfq** cannot be recognized as fully satisfying because the **tfq** molecules are engaged in HBs with substrate **4**. Thus, we tried cocrystallization with **ofn**, which afforded cocrystal **4**$_2$·**ofn** (triclinic space group $P\bar{1}$) again with a 2:1 stoichiometry. Its crystal structure revealed the anticipated lactam dimers **V** that, in contrast to **4**$_2$·**tfq**, are essentially planar. The **4**$_2$ dimers and **ofn** molecules are coplanar and connected by means of C—H···F interactions forming flat ribbons spreading along $[30\bar{1}]$ (Figure 6a). The polymeric structures aggregate on top of each other into infinite columns stabilized by almost perfectly cofacial π−π stacking interactions (the dihedral angle between the planes of the molecules of both components is equal to 0.4°). The interplanar distances are 3.34 and 3.42 Å for aryl···perfluoroaryl and aryl···aryl interaction, respectively (Figure 6b,c). The adjacent columns are connected via additional C—H···F HBs creating a stairlike 3D architecture.

Indole-2-carboxylic Acid (5). Carboxylic acids generally crystallize as cyclic $R_2^2(8)$ hydrogen-bonded dimers **VIII**, whereas the catemer $C(4)$ motif **IX** (Scheme 5), where each carboxyl group is linked to two neighbors via single O—H···O=C HBs, is rarely encountered in the solid state.[83,84]

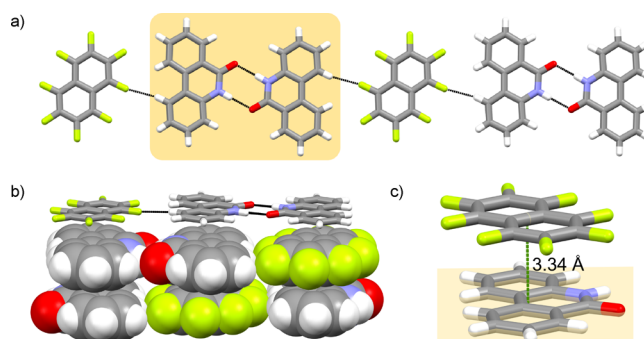**Figure 6.** Crystal structure of **4**$_2$·**ofn**: (a) top view of a fragment of the ribbon composed of alternating lactam dimers and **ofn** molecules (one of the dimers is highlighted in light orange), (b) side view of the molecules stacked in a brick-wall motif, and (c) view of the relative orientation of the molecules of **ofn** and **4** with the distance between the centroid of **ofn** and the plane of **4**. HBs are indicated by black lines.

Scheme 5. Most Frequent Supramolecular Motifs VIII−IX Found in Crystal Structures of Carboxylic Acids and the Schematic Representation of the Crystal Structure of Uncomplexed 5 (Motif X)
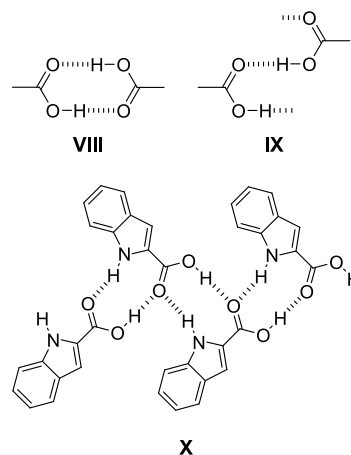
Usually, weaker C—H···O or C—H···N interactions are necessary to stabilize the catemer motif.[85−88] A prominent example is indole-2-carboxylic acid (**5**), which attracts increasing interest in various biological activities.[89,90] The crystal structure of **5** exhibits parallel layers composed of catemers **X** stabilized by additional N—H···O HBs (Scheme 5).[89] Because the acid does not crystallize with **hfb**, we tried cocrystallization with pentafluorobenzoic acid (**pfba**) in the expectation that stacking interactions with the cyclic homodimers of **pfba** may induce dimeric self-assembly of **5**. Obviously, the success of this experiment relied on the formation of homodimers. However, benzoic acids generally exhibit the opposite tendency and prefer creation of heterodimers by 1 kcal·mol^{-1} for a pair of aromatic carboxylic acids with substituents of different electronegativities.[42,91] Cocrystallization of the components from CH$_2$Cl$_2$ furnished a 2:1 cocrystal, **5**$_2$·**pfba**, and fortunately, the X-ray analysis revealed that the crystals (the triclinic space group $P\bar{1}$) are composed of centrosymmetric homodimers of **pfba** and noncentrosymmetric dimers of **5**. The dimers of **5** are essentially planar, whereas in **pfba** dimers, because of the steric hindrance, the carboxyl groups are twisted by ca. 43°
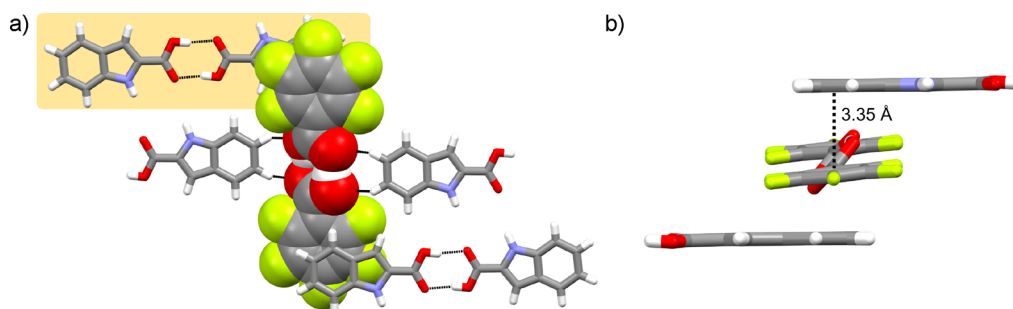
Figure 7. Crystal structure of $\mathbf{5_2}\cdot\mathbf{pfba}$: (a) top view of a fragment of the structure showing the relative orientation of the homodimers of **5** and **pfba** (one of the $\mathbf{5_2}$ dimers is highlighted in light orange) and (b) π-stacked homodimers with the distance between the centroid of the pentafluorophenyl unit and the plane of **5** (view along the plane of a molecule of **5**). HBs are indicated by black lines.
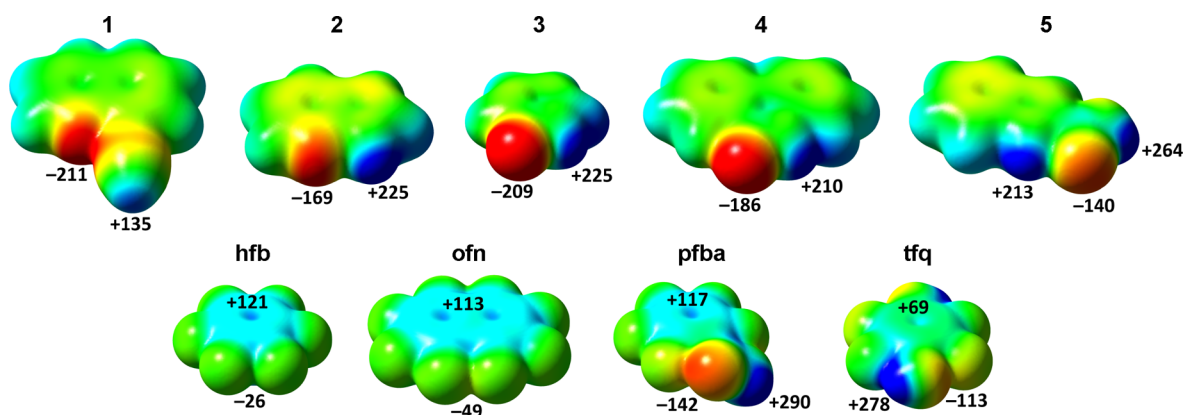

Figure 8. Electrostatic potential (ESP) surfaces of compounds **1**−**5** and the perfluoroaryls **hfb**, **ofn**, **pfba**, and **tfq** mapped on the molecular ρ = 0.002 au isosurface of electron density. Color ranges from −0.06 (red) to +0.06 au (blue). Selected most positive ($V_{S,max}$) and most negative ($V_{S,min}$) ESP values (in kJ/mol) are indicated.

from the plane of the pentafluorophenyl rings. The homodimers of these components are perpendicularly oriented in such a way that the pentafluorophenyl rings of each **pfba** dimer stack onto the phenyl rings of two different dimers of **5** and *vice versa*. They are further aggregated through C_{Ar}−H···O HBs between the aryl moiety of one of the symmetrically inequivalent molecules of **5** and two oxygen atoms of the **pfba** dimer (Figure 7a, Table 1). As in $\mathbf{3_2}\cdot\mathbf{tfq}$, the molecules of both components are stacked in an offset $(DCC)_n$ pattern. The perfluorinated rings of the **pfba** (D) molecules and the molecules of **5** (C) are not parallel to each other; the dihedral angle between the planes of the aryl and perfluoroaryl moieties is about 6.5°. The distance between the centroid of the pentafluorophenyl ring and the plane of **5** is equal to 3.35 Å. Furthermore, because of the aryl−perfluoroaryl interactions, the strong N−H···O HBs (present in the crystal structure of the uncomplexed **5**) were broken, and the N−H HB donor in the cocrystal does not form any contacts with the neighboring molecules (even though it remains in close proximity to a carbonyl oxygen atom).

Electrostatic Potential Maps. The formation of hydrogen bonds and other noncovalent interactions is mainly the result of electrostatic forces operating between electron-rich and electron-deficient regions of a molecule that, in turn, are associated with the presence of a negative or positive electrostatic potential around a particular atom, respectively.[92] Therefore, DFT calculations of the electrostatic potential (ESP) have been performed for all nine compounds investigated in this study. Figure 8 represents the ESP maps, where the red color depicts the most electron-rich regions of a

molecule (negative electrostatic potential), whereas the blue color indicates the most electron-deficient regions of a molecule (positive electrostatic potentials). The molecular regions of low electronic density and positive electrostatic potential perpendicular to the plane of the aromatic π-regions can be treated as π-holes that are responsible for intermolecular interactions with negative sites like π-electrons or lone pairs.[29,30]

The ESP maps indicate that the sp^2 pyridine nitrogen atom is the most electron-rich region in molecules **1** and **2**. The magnitude of the local minimum of the electrostatic potential at the pyridine nitrogen atom in **1** ($V_{S,min}$ = −211 kJ/mol) is about 40 kJ/mol lower compared to **2** (−169 kJ/mol), suggesting that the nitrogen atom in 8-ethynylquinoline is a significantly better acceptor of the hydrogen bond than the pyridine nitrogen atom in 7-azaindole. In turn, the most positive electrostatic potential region in **1** is localized at the acetylene hydrogen atom ($V_{S,max}$ = +135) and at the N−H proton ($V_{S,max}$ = +225 kJ/mol) in **2**, clearly showing the better HB donor ability of the N−H fragment. Moreover, the area of the repulsive potential extends to the C−H proton adjacent to the N−H moiety in the pyrrole ring of **2**. The presence of such areas is strictly in line with the geometric preferences of N−H···N and C−H···F HBs in the $\mathbf{2_2}\cdot\mathbf{hfb}$ cocrystal. Electrostatic potential maps of lactams **3** and **4** leave no doubt that the attractive potential is concentrated on the carbonyl oxygen atom (−209 and −186 kJ/mol respectively), whereas the repulsive potential is mainly localized on the hydrogen atom of the amide moiety. Such a distribution of the potential successfully explains the presence of self-complementary

lactam dimers in 3_2·hfb and 4_2·ofn cocrystals. The N−H···O═C HBs that connect the lactam molecules are the result of the interaction between the regions with the minimum and maximum ESP value. It was also noted that the most intense blue color on the ESP map of 3 present at the amide hydrogen atom extended toward the adjacent hydrogen atom (C−H), predicting that it too may be involved in an electrostatic interaction. And, indeed, there are short C−H···O contacts between 2-pyridone dimers in 3_2·hfb. Somewhat surprisingly, on the ESP map of 4, there is also a weak positive local maximum located between the two bay hydrogen atoms (opposite to the amide group; see Figure S2 in the ESI). This is due to the flat geometry of 4 causing the two hydrogens to overlap, which increases the local ESP. This region of the molecule is indeed involved in the C−H···F interaction in the 4_2·ofn cocrystal. Similarly, the ESP map of indole-2-carboxylic acid 5 clearly establishes the presence of a negative electrostatic potential area around the carbonyl oxygen atom and two positive regions of the O−H and N−H protons. Predictably, the higher potential (about 50 kJ/mol) is located on the carboxylic hydrogen atom.

In the case of the perfluoroaryls hfb and ofn that were used as components to facilitate the dimer formation, the differences between the $V_{S,max}$ and $V_{S,min}$ values are not as great as those in compounds 1−5. As expected, the electrostatic potential below and above the aromatic rings of hfb and ofn, loaded with electron-withdrawing fluorine atoms, is positive (in contrast with most aromatic systems). These centers of positive potential (π-holes) serve as partners in attractive $\pi-\pi$ interactions between the aryl and perfluoroaryl units. The ESP on the periphery of the molecules is only slightly negative (−26 and −49 kJ/mol for hfb and ofn, respectively). The ESP values are comparable to those reported earlier.[93,94] Two local minima of the electrostatic potential are present on the ESP map of pfba. As expected, the most negative value is present on the carbonyl oxygen atom. The most intense blue color (corresponding to $V_{S,max}$ = 290 kJ/mol) is present on the hydrogen atom of the carboxylic group, indicating the area most prone to HB formation (as in the 5_2·pfba cocrystal). Tetrafluorohydroquinone tfq is the only molecule whose potential above and below the aromatic ring is not as high as those in the other perfluorinated compounds, which can be attributed to the presence of strong electron-donating groups. On the other hand, the $V_{S,max}$ value clearly indicates that the O−H proton is a very strong hydrogen bond donor, which promotes its cocrystallization with (strong or moderate) hydrogen bond acceptors. That is why the strong O−H···O═C HBs are present in the crystal structure of 4_2·tfq.

CONCLUSIONS

We described a selection of organic compounds that are capable of forming self-complementary hydrogen bonds but, due to the packing forces, crystallizing as catemers or creating more complex crystal structures and then compared them with the results obtained from their complexation with perfluoroaryl compounds. In all the described cases, the $\pi-\pi$ stacking interactions resulted in reorganization of hydrogen bonds and induced the creation of the expected self-complementary synthons. This is apparently due to the fact that most of the catemer structures are not planar, whereas self-complementary synthons expected for the compounds studied require a coplanar orientation of the contributing molecules, which is, in turn, forced by the effective face-to-face aryl−perfluoroaryl

stacking interaction between the components constituting the complex. In summary, our results show that the aryl−perfluoroaryl $\pi-\pi$ stacking interactions show significant potential for the control of molecular self-assembly of aromatic compounds able to form hydrogen bonds. The results also demonstrate that the addition of a perfluorinated component often induces the formation of a two-component system with a layered structure. In addition, the calculated electrostatic potential surfaces correlate with the intermolecular interactions within the crystals and thus shed some light on their nature.

■ ASSOCIATED CONTENT

ⓢ Supporting Information

The Supporting Information is available free of charge at https://pubs.acs.org/doi/10.1021/acs.cgd.3c00676.

> Details on the synthesis and characterization of the cocrystals, the crystallographic data and details of the structural refinement, and description of the crystal structure of 4 (PDF)

Accession Codes

CCDC 2263874, 2263877−2263878, 2263881, 2263886, 2263888, and 2263893−2263894 contain the supplementary crystallographic data for this paper. These data can be obtained free of charge via www.ccdc.cam.ac.uk/data_request/cif, or by emailing data_request@ccdc.cam.ac.uk, or by contacting The Cambridge Crystallographic Data Centre, 12 Union Road, Cambridge CB2 1EZ, UK; fax: +44 1223 336033. Crystallographic data reported in this paper have been deposited with the Cambridge Crystallographic Data Centre as supplementary publication no. CCDC 2263874 (1), 2263877 (3_2·hfb), 2263878 (5_2·pfba), 2263881 (4), 2263886 (4_2·tfq), 2263888 (1_2·hfb), 2263893 (4_2·ofn), and 2263894 (2_2·hfb). The data can be obtained free of charge from The Cambridge Crystallographic Data Centre via www.ccdc.cam.ac.uk/structures.

■ AUTHOR INFORMATION

Corresponding Author

Teresa Olszewska − Department of Organic Chemistry, Faculty of Chemistry, Gdańsk University of Technology, Gdańsk 80-233, Poland; ⓞ orcid.org/0000-0003-1477-1562; Phone: +48 58 347 14 25; Email: teresa.olszewska@pg.edu.pl

Authors

Jan Alfuth − Department of Organic Chemistry, Faculty of Chemistry, Gdańsk University of Technology, Gdańsk 80-233, Poland; ⓞ orcid.org/0000-0003-3428-5705

Katarzyna Kazimierczuk − Department of Inorganic Chemistry, Faculty of Chemistry, Gdańsk University of Technology, Gdańsk 80-233, Poland; ⓞ orcid.org/0000-0002-0821-376X

Tadeusz Połoński − Department of Organic Chemistry, Faculty of Chemistry, Gdańsk University of Technology, Gdańsk 80-233, Poland; ⓞ orcid.org/0000-0003-2994-7954

Complete contact information is available at:
https://pubs.acs.org/10.1021/acs.cgd.3c00676

Author Contributions

The manuscript was written through contributions of all authors. All authors have given approval to the final version of the manuscript.

Notes

The authors declare no competing financial interest.

■ REFERENCES

(1) Desiraju, G. R. Crystal Engineering. *The Design of Organic Solids*; Elsevier: Amsterdam, 1989.

(2) Desiraju, G. R. *The Crystal as a Supramolecular Entity*; Wiley: Chichester, 1995.

(3) Lehn, J.-M. *Supramolecular Chemistry: Concepts and Perspectives*; Wiley-VCH: Weinheim, 1995.

(4) Jones, W. *Organic Molecular Solids: Properties and Applications*; Jones, W., Ed.; CRC Press: Boca Raton, 1997.

(5) Chin, D. N.; Zerkowski, J. A.; MacDonald, J. C.; Whitesides, G. M. Strategies for the Design and Assembly of Hydrogen-Bonded Aggregates in the Solid State. In *Organised Molecular Assemblies in the Solid State*; Whitesell, J. K., Ed.; Wiley: Chichester, 1999; 185.

(6) Moulton, B.; Zaworotko, M. J. From Molecules to Crystal Engineering: Supramolecular Isomerism and Polymorphism in Network Solids. *Chem. Rev.* **2001**, *101*, 1629−1658.

(7) Aakeröy, C. B.; Seddon, K. R. The Hydrogen Bond and Crystal Engineering. *Chem. Soc. Rev.* **1993**, *22*, 397−407.

(8) MacDonald, J. C.; Whitesides, G. M. Solid-State Structures of Hydrogen-Bonded Tapes Based on Cyclic Secondary Diamides. *Chem. Rev.* **1994**, *94*, 2383−2420.

(9) Su, D.; Wang, X.; Simard, M.; Wuest, J. D. Molecular Tectonics. *Supramol. Chem.* **1995**, *6*, 171−178.

(10) Fredericks, J. R.; Hamilton, A. D. *Comprehensive Supramolecular Chemistry*; Atwood, J. L., Davis, J. E. D., MacNicol, D. D., Vögtle, F., Eds.; Pergamon: Oxford, 1996; Vol. 9, 565.

(11) Coe, S.; Kane, J. J.; Nguyen, T. L.; Toledo, L. M.; Wininger, E.; Fowler, F. W.; Lauher, J. W. Molecular Symmetry and the Design of Molecular Solids: The Oxalamide Functionality as a Persistent Hydrogen Bonding Unit. *J. Am. Chem. Soc.* **1997**, *119*, 86−93.

(12) Meléndez, R. E.; Hamilton, A. D. Hydrogen-Bonded Ribbons, Tapes and Sheets as Motifs for Crystal Engineering. In *Design of Organic Solids*; Weber, E., Ed.; Springer, 1998; 97−129.

(13) Archer, E. A.; Gong, H.; Krische, M. J. Hydrogen Bonding in Noncovalent Synthesis: Selectivity and the Directed Organization of Molecular Strands. *Tetrahedron* **2001**, *57*, 1139−1159.

(14) Desiraju, G. R. Supramolecular Synthons in Crystal Engineering—A New Organic Synthesis. *Angew. Chem., Int. Ed.* **1995**, *34*, 2311−2327.

(15) Desiraju, G. R. Designer Crystals: Intermolecular Interactions, Network Structures and Supramolecular Synthons. *Chem. Commun.* **1997**, *28*, 1475−1482.

(16) Sherrington, D. C.; Taskinen, K. A. Self-Assembly in Synthetic Macromolecular Systems via Multiple Hydrogen Bonding Interactions. *Chem. Soc. Rev.* **2001**, *30*, 83−93.

(17) Hunter, C. A. The Role of Aromatic Interactions in Molecular Recognition. *Chem. Soc. Rev.* **1994**, *23*, 101−109.

(18) Hunter, C. A.; Lawson, K. R.; Perkins, J.; Urch, C. J. Aromatic Interactions. *J. Chem. Soc., Perkin Trans.* **2001**, *2*, 651−669.

(19) Janiak, C. A Critical Account on π-π Stacking in Metal Complexes with Aromatic Nitrogen-Containing Ligands. *J. Chem. Soc. Dalt. Trans.* **2000**, 3885−3896.

(20) Thakuria, R.; Nath, N. K.; Saha, B. K. The Nature and Applications of π-π Interactions: A Perspective. *Cryst. Growth Des.* **2019**, *19*, 523−528.

(21) Martinez, C. R.; Iverson, B. L. Rethinking the Term "Pi-Stacking. *Chem. Sci.* **2012**, *3*, 2191−2201.

(22) Hwang, J.; Li, P.; Shimizu, K. D. Synergy between Experimental and Computational Studies of Aromatic Stacking Interactions. *Org. Biomol. Chem.* **2017**, *15*, 1554−1564.

(23) Patrick, C. R.; Prosser, G. S. A Molecular Complex of Benzene and Hexafluorobenzene. *Nature* **1960**, *187*, 1021−1021.

(24) Gavezzotti, A. On the Preferred Mutual Orientation of Aromatic Groups in Organic Condensed Media. *Chem. Phys. Lett.* **1989**, *161*, 67−72.

(25) Bacchi, S.; Benaglia, M.; Cozzi, F.; Demartin, F.; Filippini, G.; Gavezzotti, A. X-Ray Diffraction and Theoretical Studies for the Quantitative Assessment of Intermolecular Arene-Perfluoroarene Stacking Interactions. *Chem. Eur. J.* **2006**, *12*, 3538−3546.

(26) Williams, J. H. The Molecular Electric Quadrupole Moment and Solid-State Architecture. *Acc. Chem. Res.* **1993**, *26*, 593−598.

(27) Lorenzo, S.; Lewis, G. R.; Dance, I. Supramolecular Potentials and Embraces for Fluorous Aromatic Molecules. *New J. Chem.* **2000**, *24*, 295−304.

(28) Hernández-Trujillo, J.; Colmenares, F.; Cuevas, G.; Costas, M. MP2 Ab Initio Calculations of the Hexafluorobenzene-Benzene and -Monofluorobenzene Complexes. *Chemical Physics Letters* **1997**, *265*, 503−507.

(29) Bauzá, A.; Mooibroek, T. J.; Frontera, A. The Bright Future of Unconventional σ/π-Hole Interactions. *ChemPhysChem* **2015**, *16*, 2496−2517.

(30) Politzer, P.; Murray, J. S.; Clark, T. The π-Hole Revisited. *Phys. Chem. Chem. Phys.* **2021**, *23*, 16458−16468.

(31) Klosterman, J. K.; Fujita, M.; Yamauchi, Y. Engineering Discrete Stacks of Aromatic Molecules. *Chem. Soc. Rev.* **2009**, *38*, 1714−1725.

(32) Sharada, D.; Saraswatula, V. G.; Saha, B. K. Steering the Host Network from Cage to Channel by π···π Interactions among the Guest Molecules. *Cryst. Growth Des.* **2018**, *18*, 3719−3723.

(33) Hashim, M. I.; Le, H. T. M.; Chen, T. H.; Chen, Y. S.; Daugulis, O.; Hsu, C. W.; Jacobson, A. J.; Kaveevivitchai, W.; Liang, X.; Makarenko, T.; Miljanić, O. Š.; Popovs, I.; Tran, H. V.; Wang, X.; Wu, C. H.; Wu, J. I. Dissecting Porosity in Molecular Crystals: Influence of Geometry, Hydrogen Bonding, and [π···π] Stacking on the Solid-State Packing of Fluorinated Aromatics. *J. Am. Chem. Soc.* **2018**, *140*, 6014−6026.

(34) Reichenbächer, K.; Süss, H. I.; Hulliger, J. Fluorine in Crystal Engineering—"the Little Atom That Could". *Chem. Soc. Rev.* **2005**, *34*, 22−30.

(35) Collings, J. C.; Roscoe, K. P.; Thomas, R. L.; Batsanov, A. S.; Stimson, L. M.; Howard, J. A. K.; Marder, T. B. Arene-Perfluoroarene Interactions in Crystal Engineering. Part 3. Single-Crystal Structures of 1:1 Complexes of Octafluoronaphthalene with Fused-Ring Polyaromatic Hydrocarbons. *New J. Chem.* **2001**, *25*, 1410−1417.

(36) Smith, C. E.; Smith, P. S.; Thomas, R. L.; Robins, E. G.; Collings, J. C.; Dai, C.; Scott, A. J.; Borwick, S.; Batsanov, A. S.; Watt, S. W.; Clark, S. J.; Viney, C.; Howard, J. A. K.; Clegg, W.; Marder, T. B. Arene-Perfluoroarene Interactions in Crystal Engineering: Structural Preferences in Polyfluorinated Tolans. *J. Mater. Chem.* **2004**, *14*, 413−420.

(37) Serrano-Becerra, J. M.; Hernández-Ortega, S.; Morales-Morales, D.; Valdés-Martínez, J. Bottom-up Design and Construction of a Non-Centrosymmetric Network through π−π Stacking Interactions. *CrystEngComm* **2009**, *11*, 226−228.

(38) Cozzi, F.; Bacchi, S.; Filippini, G.; Pilati, T.; Gavezzotti, A. Synthesis, X-Ray Diffraction and Computational Study of the Crystal Packing of Polycyclic Hydrocarbons Featuring Aromatic and Perfluoroaromatic Rings Condensed in the Same Molecule: 1,2,3,4-Tetrafluoronaphthalene, -Anthracene and -Phenanthrene. *Chem. Eur. J.* **2007**, *13*, 7177−7184.

(39) Sergeyev, S.; Pisula, W.; Geerts, Y. H. Discotic Liquid Crystals: A New Generation of Organic Semiconductors. *Chem. Soc. Rev.* **2007**, *36*, 1902−1929.

(40) Ni, B. B.; Wang, C.; Wu, H.; Pei, J.; Ma, Y. Copper-Free Cycloaddition of Azide and Alkyne in Crystalline State Facilitated by Arene-Perfluoroarene Interactions. *Chem. Commun.* **2010**, *46*, 782−784.

(41) Chen, T.; Li, M.; Liu, J. π-π Stacking Interaction: A Nondestructive and Facile Means in Material Engineering for Bioapplications. *Cryst. Growth Des.* **2018**, *18*, 2765−2783.

(42) Gdaniec, M.; Jankowski, W.; Milewska, M. J.; Połoński, T. Supramolecular Assemblies of Hydrogen-Bonded Carboxylic Acid Dimers Mediated by Phenyl-Pentafluorophenyl Stacking Interactions. *Angew. Chem. Int. Ed.* **2003**, *42*, 3903−3906.

(43) Yamasaki, R.; Iida, M.; Ito, A.; Fukuda, K.; Tanatani, A.; Kagechika, H.; Masu, H.; Okamoto, I. Crystal Engineering of N,N′-Diphenylurea Compounds Featuring Phenyl-Perfluorophenyl Interaction. *Cryst. Growth Des.* **2017**, *17*, 5858−5866.

(44) Albrecht, M.; Yi, H.; Pan, F.; Valkonen, A.; Rissanen, K. Connecting Electron-Deficient and Electron-Rich Aromatics to Support Intermolecular Interactions in Crystals. *Eur. J. Org. Chem.* **2015**, *2015*, 3235−3239.

(45) Althagbi, H. I.; Edwards, A. J.; Nicholson, B. K.; Reason, D. A.; Saunders, G. C.; Sim, S. A.; Van Der Heijden, D. A. Arene-Perfluoroarene-Anion Stacking and Hydrogen Bonding Interactions in Imidazolium Salts for the Crystal Engineering of Polarity. *Cryst. Growth Des.* **2016**, *16*, 174−188.

(46) Bhandary, S.; Chopra, D. Assessing the Significance of Hexafluorobenzene as a Unique Guest Agent through Stacking Interactions in Substituted Ethynylphenyl Benzamides. *Cryst. Growth Des.* **2018**, *18*, 3027−3036.

(47) Molčanov, K.; Milašinović, V.; Kojić-Prodić, B. Contribution of Different Crystal Packing Forces in π-Stacking: From Noncovalent to Covalent Multicentric Bonding. *Cryst. Growth Des.* **2019**, *19*, 5967−5980.

(48) Cozzi, F.; Bacchi, S.; Filippini, G.; Pilati, T.; Gavezzotti, A. Competition between Hydrogen Bonding and Arene-Perfluoroarene Stacking. X-Ray Diffraction and Molecular Simulation on 5,6,7,8-Tetrafluoro-2-Naphthoic Acid and 5,6,7,8-Tetrafluoro-2-Naphthamide Crystals. *CrystEngComm* **2009**, *11*, 1122−1127.

(49) Campillo-Alvarado, G.; Li, C.; Swenson, D. C.; Macgillivray, L. R. Application of Long-Range Synthon Aufbau Modules Based on Trihalophenols to Direct Reactivity in Binary Cocrystals: Orthogonal Hydrogen Bonding and π-π Contact Driven Self-Assembly with Single-Crystal Reactivity. *Cryst. Growth Des.* **2019**, *19*, 2511−2518.

(50) Philips, D. S.; Kartha, K. K.; Politi, A. T.; Krüger, T.; Albuquerque, R. Q.; Fernández, G. Interplay between H-Bonding and Preorganization in the Evolution of Self-Assembled Systems. *Angew. Chem. Int. Ed.* **2019**, *58*, 4732−4736.

(51) Nisbet, M. L.; Wang, Y.; Poeppelmeier, K. R. Symmetry-Dependent Intermolecular π−π Stacking Directed by Hydrogen Bonding in Racemic Copper-Phenanthroline Compounds. *Cryst. Growth Des.* **2021**, *21*, 552−562.

(52) Yee, N.; Dadvand, A.; Hamzehpoor, E.; Titi, H. M.; Perepichka, D. F. Hydrogen Bonding Versus π-Stacking in Charge-Transfer Co-Crystals. *Cryst. Growth Des.* **2021**, *21*, 2609−2613.

(53) Alfuth, J.; Chojnacki, J.; Połoński, T.; Herman, A.; Milewska, M. J.; Olszewska, T. Interplay between Aryl···Perfluoroaryl and Hydrogen Bonding Interactions in Cocrystals of Pentafluorophenol with Molecules of Trigonal Symmetry. *Cryst. Growth Des.* **2022**, *22*, 3493−3504.

(54) Greco, N. J.; Hysell, M.; Goldenberg, J. R.; Rheingold, A. L.; Tor, Y. Alkyne-Containing Chelating Ligands: Synthesis, Properties and Metal Coordination of 1,2-Di(Quinolin-8-yl)Ethyne. *Dalton Trans.* **2006**, 2288−2290.

(55) Smith, P. A. S. The Schmidt Reaction: Experimental Conditions and Mechanism. *J. Am. Chem. Soc.* **1948**, *70*, 320−323.

(56) Frisch, M. J.; Trucks, G. W.; Schlegel, H. B.; Scuseria, G. E.; Robb, M. A.; Cheeseman, J. R.; Scalmani, G.; Barone, V.; Petersson, G. A.; Nakatsuji, H.; Li, X.; Caricato, M.; Marenich, A. V.; Bloino, J.; Janesko, B. G.; Gomperts, R.; Mennucci, B.; Hratchian, H. P.; Ortiz, J. V.; Izmaylov, A. F.; Sonnenberg, J. L.; Williams-Young, D.; Ding, F.; Lipparini, F.; Egidi, F.; Goings, J.; Peng, B.; Petrone, A.; Henderson, T.; Ranasinghe, D.; Zakrzewski, V. G.; Gao, J.; Rega, N.; Zheng, G.; Liang, W.; Hada, M.; Ehara, M.; Toyota, K.; Fukuda, R.; Hasegawa, J.; Ishida, M.; Nakajima, T.; Honda, Y.; Kitao, O.; Nakai, H.; Vreven, T.;

Throssell, K.; Montgomery, Jr., J. A.; Peralta, J. E.; Ogliaro, F.; Bearpark, M. J.; Heyd, J. J.; Brothers, E. N.; Kudin, K. N.; Staroverov, V. N.; Keith, T. A.; Kobayashi, R.; Normand, J.; Raghavachari, K.; Rendell, A. P.; Burant, J. C.; Iyengar, S. S.; Tomasi, J.; Cossi, M.; Millam, J. M.; Klene, M.; Adamo, C.; Cammi, R.; Ochterski, J. W.; Martin, R. L.; Morokuma, K.; Farkas, O.; Foresman, J. B.; Fox, D. J. *Gaussian 16* (Revision C.01); Gaussian, Inc.: Wallingford CT, 2019.

(57) Dennington, R. D.; Keith, T. A.; Millam, J. M. *GaussView*, Version 6.1.1; Semichem Inc.: Shawnee Mission, KS, 2019.

(58) STOE &Cie GmbH *X-Area 1.75*; STOE &Cie GmbH: Darmstadt, Germany, 2015.

(59) Sheldrick, G. M. SHELXT − Integrated Space-Group and Crystal-Structure Determination. *Acta Crystallogr., Sect. A* **2015**, *71*, 3−8.

(60) Sheldrick, G. M. Crystal Structure Refinement with SHELXL. *Acta Crystallogr. Sect. C* **2015**, *71*, 3−8.

(61) Westrip, S. P. PublCIF: Software for Editing, Validating and Formatting Crystallographic Information Files. *J. Appl. Crystallogr.* **2010**, *43*, 920−925.

(62) Dolomanov, O. V.; Bourhis, L. J.; Gildea, R. J.; Howard, J. A. K.; Puschmann, H. OLEX2: A Complete Structure Solution, Refinement and Analysis Program. *J. Appl. Crystallogr.* **2009**, *42*, 339−341.

(63) Macrae, C. F.; Sovago, I.; Cottrell, S. J.; Galek, P. T. A.; McCabe, P.; Pidcock, E.; Platings, M.; Shields, G. P.; Stevens, J. S.; Towler, M.; Wood, P. A. Mercury 4.0: From Visualization to Analysis, Design and Prediction. *J. Appl. Crystallogr.* **2020**, *53*, 226−235.

(64) Ohkita, M.; Suzuki, T.; Nakatani, K.; Tsuji, T. Crystal Engineering Using Very Short and Linear C(sp)-H···N Hydrogen Bonds: Formation of Head-to-Tail Straight Tapes and Their Assembly into Nonlinear Optical Polar Crystals. *Chem. Commun.* **2001**, *1*, 1454−1455.

(65) Ohkita, M.; Kawano, M.; Suzuki, T.; Tsuji, T. Supramolecular Graphyne: A C(sp)-H···N Hydrogen-Bonded Unique Network Structure of 2,4,6-Triethynyl-1,3,5-Triazine. *Chem. Commun.* **2002**, 3054−3055.

(66) Kirchner, M. T.; Boese, R.; Gehrke, A.; Bläser, D. Co-Crystallization with Acetylene. Part III. Molecular Complexes with Aromatic Azacycles. *CrystEngComm* **2004**, *6*, 360−366.

(67) West, K.; Wang, C.; Batsanov, A. S.; Bryce, M. R. Are Terminal Aryl Butadiynes Stable? Synthesis and X-Ray Crystal Structures of a Series of Aryl- and Heteroaryl-Butadiynes (Ar−C≡C−C≡C−H). *J. Org. Chem.* **2006**, *71*, 8541−8544.

(68) Bosch, E. Role of sp-C−H···N Hydrogen Bonding in Crystal Engineering. *Cryst. Growth Des.* **2010**, *10*, 3808−3813.

(69) Bosch, E. Comparison of sp-C−H···N Hydrogen Bond Lengths in Fluorinated and Nonfluorinated Ethynylbenzenes. *J. Chem. Crystallogr.* **2014**, *44*, 287−292.

(70) Thalladi, V. R.; Weiss, H. C.; Bläser, D.; Boese, R.; Nangia, A.; Desiraju, G. R. C-H···F Interactions in the Crystal Structures of Some Fluorobenzenes. *J. Am. Chem. Soc.* **1998**, *120*, 8702−8710.

(71) Bondi, A. Van Der Waals Volumes and Radii. *J. Phys. Chem.* **1964**, *68*, 441−451.

(72) Zhao, S.-B.; Wang, S. Luminescence and Reactivity of 7-Azaindole Derivatives and Complexes. *Chem. Soc. Rev.* **2010**, *39*, 3142−3156.

(73) Kannaboina, P.; Mondal, K.; Laha, J. K.; Das, P. Recent Advances in the Global Ring Functionalization of 7-Azaindoles. *Chem. Commun.* **2020**, *56*, 11749−11762.

(74) Walmsley, J. A. Self-Association of 7-Azaindole in Nonpolar Solvents. *J. Phys. Chem.* **1981**, *85*, 3181−3187.

(75) Fiebig, T.; Chachisvilis, M.; Manger, M.; Zewail, A. H.; Douhal, A.; Garcia-Ochoa, I.; de La Hoz Ayuso, A. Femtosecond Dynamics of Double Proton Transfer in a Model DNA Base Pair: 7-Azaindole Dimers in the Condensed Phase. *J. Phys. Chem. A* **1999**, *103*, 7419−7431.

(76) Kwon, O.-H.; Zewail, A. H. Double Proton Transfer Dynamics of Model DNA Base Pairs in the Condensed Phase. *Proc. Natl. Acad. Sci. U. S. A.* **2007**, *104*, 8703−8708.

(77) Dufour, P.; Dartiguenave, Y.; Dartiguenave, M.; Dufour, N.; Lebuis, A. M.; Bélanger-Gariépy, F.; Beauchamp, A. L. Crystal Structures of 7-Azaindole, an Unusual Hydrogen-Bonded Tetramer, and of Two of Its Methylmercury(II) Complexes. *Can. J. Chem.* **1990**, *68*, 193−201.

(78) Bedeković, N.; Fotović, L.; Stilinović, V.; Cinčić, D. Conservation of the Hydrogen-Bonded Pyridone Homosynthon in Halogen-Bonded Cocrystals. *Crystal Growth Des.* **2022**, *22*, 987−992.

(79) Penfold, B. R. The Electron Distribution in Crystalline α-Pyridone. *Acta Crystallogr.* **1953**, *6*, 591−600.

(80) Yang, H. W.; Craven, B. M. Charge Density Study of 2-Pyridone. *Acta Crystallogr. Sect. B* **1998**, *54*, 912−920.

(81) Arman, H. D.; Poplaukhin, P.; Tiekink, E. R. T. 2-Pyridone: Monoclinic Polymorph. *Acta Crystallogr. Sect. E* **2009**, *65*, o3187−o3187.

(82) Sen, D.; Crystal, K. Molecular Structure of Phenanthridone. *Acta Crystallogr. Sect. B* **1970**, *26*, 1629−1630. Due to the high R-factor of the structure, we decided to determine it again. The obtained result is identical to the published one and is presented in ESI.

(83) Leiserowitz, L. Molecular Packing Modes. Carboxylic Acids. *Acta Crystallogr. Sect. B* **1976**, *32*, 775−802.

(84) Frankenbach, G. M.; Etter, M. C. Relationship between Symmetry in Hydrogen-Bonded Benzoic Acids and the Formation of Acentric Crystal Structures. *Chem. Mater.* **1992**, *4*, 272−278.

(85) Moorthy, J. N.; Natarajan, R.; Mal, P.; Venugopalan, P. Helical Self-Assembly of Substituted Benzoic Acids: Influence of Weaker X··· X and C−H···X Interactions. *J. Am. Chem. Soc.* **2002**, *124*, 6530−6531.

(86) Desiraju, G. R. C−H···O and Other Weak Hydrogen Bonds. From Crystal Engineering to Virtual Screening. *Chem. Commun.* **2005**, 2995−3001.

(87) Das, D.; Desiraju, G. R. Packing Modes in Some Mono- and Disubstituted Phenylpropiolic Acids: Repeated Occurrence of the Rare syn,anti Catemer. *Chem. - Asian J.* **2006**, *1*, 231−244.

(88) Sanphui, P.; Bolla, G.; Das, U.; Mukherjee, A. K.; Nangia, A. Acemetacin Polymorphs: A Rare Case of Carboxylic Acid Catemer and Dimer Synthons. *CrystEngComm* **2013**, *15*, 34−38.

(89) Morzyk-Ociepa, B.; Michalska, D.; Pietraszko, A. Structures and Vibrational Spectra of Indole Carboxylic Acids. Part I. Indole-2-Carboxylic Acid. *J. Mol. Struct.* **2004**, *688*, 79−86.

(90) Cui, G.; Lai, F.; Wang, X.; Chen, X.; Xu, B. Design, Synthesis and Biological Evaluation of Indole-2-Carboxylic Acid Derivatives as IDO1/TDO Dual Inhibitors. *Eur. J. Med. Chem.* **2020**, *188*, No. 111985.

(91) Sharma, C. V. K.; Panneerselvam, K.; Pilati, T.; Desiraju, G. R. Molecular Recognition Involving an Interplay of O−H···O, C−H···O and π···π Interactions. The Anomalous Crystal Structure of the 1:1 Complex 3,5-Dinitrobenzoic Acid−4-(*N*,*N*-Dimethylamino)Benzoic Acid. *J. Chem. Soc., Perkin Trans.* **1993**, *2*, 2209−2216.

(92) Politzer, P.; Murray, J. S. Quantitative Analyses of Molecular Surface Electrostatic Potentials in Relation to Hydrogen Bonding and Co-Crystallization. *Cryst. Growth Des.* **2015**, *15*, 3767−3774.

(93) Wheeler, S. E.; Houk, K. N. Through-Space Effects of Substituents Dominate Molecular Electrostatic Potentials of Substituted Arenes. *J. Chem. Theory Comput.* **2009**, *5*, 2301−2312.

(94) Aliakbar Tehrani, Z.; Kim, K. S. Functional Molecules and Materials by π-Interaction Based Quantum Theoretical Design. *Int. J. Quantum Chem.* **2016**, *116*, 622−633.

📖 Recommended by ACS

New Aspects of Alcohol–Alcohol and Alcohol–Water Interactions: Crystallographic and Quantum Chemical Studies of Antiparallel O–H/O–H Interactions

Milan R. Milovanović and Snežana D. Zarić
JANUARY 29, 2024
THE JOURNAL OF PHYSICAL CHEMISTRY LETTERS   READ 🗗

Sigma-Hole and Lone-Pair-Hole Site-Based Interactions of Seesaw Tetravalent Chalcogen-Bearing Molecules with Lewis Bases

Mahmoud A. A. Ibrahim, Tamer Shoeib, *et al.*
AUGUST 30, 2023
ACS OMEGA   READ 🗗

2,2′-Bipyridine Derivatives as Halogen Bond Acceptors in Multicomponent Crystals

Filip Kučas, Dominik Cinčić, *et al.*
NOVEMBER 09, 2023
CRYSTAL GROWTH & DESIGN   READ 🗗

Gauging the Strength of the Molecular Halogen Bond via Experimental Electron Density and Spectroscopy†

Felix Otte, Carsten Strohmann, *et al.*
JUNE 05, 2023
ACS OMEGA   READ 🗗

Get More Suggestions >